



ELSEVIER

Journal of Nuclear Materials 266–269 (1999) 462–466

Journal of
nuclear
materials

Noble gas exhaust with a strongly baffled divertor in ASDEX-Upgrade

H.-S. Bosch^{*}, W. Ullrich, A. Bard, D. Coster, G. Haas, A. Kallenbach, J. Neuhauser, R. Schneider, ASDEX Upgrade Team

Max-Planck Institut für Plasmaphysik, Euratom-IPP Association, D-85748 Garching, Germany

Abstract

Since spring of 1997 ASDEX Upgrade has operated with the new divertor II (LYRA), which is characterised by vertical target plates, tight baffling towards the main chamber, and a dome baffle in the private flux region. The main goal of this divertor modification was to increase the divertor density (of the plasma and of the neutrals) for a given plasma density, whereas the neutral density in the main chamber should be similar or even lower. Pumping occurs now from the private flux region which is linked to the pump chamber by finite conductance below the outer target. A cryo pump (about 100 m³/s) has been installed in the outer divertor chamber in addition to the turbo pumps. This divertor scheme is very similar to the one planned for ITER. First experiments with the new divertor indicate that the compression of helium, C_{He} (the ratio of neutral He density in the divertor to the He density at the plasma edge) is much higher in the new divertor, while the neon exhaust efficiency has decreased. The cryo pump can strongly enhance the scrape-off layer flow of deuterium (by a factor of about 3), resulting in a small improvement of the He exhaust rate. © 1999 Elsevier Science B.V. All rights reserved.

Keywords: ASDEX Upgrade; B2/EIRENE; Divertor; Helium exhaust; Neutral transport

1. Introduction

Since 1997, ASDEX Upgrade is operated with a new divertor, the so-called Divertor II [1] in the LYRA configuration. This divertor is characterised by vertical target plates with small angles of incidence of the field lines near the separatrix, which at the same time, further away from the separatrix, follow the flux surfaces parallel to achieve tight baffling towards the main chamber. Fig. 1 shows the previous divertor configuration (DIV-I, top) with the flat, almost horizontal target plates close to the X-point and this new configuration (DIV-II, bottom). The neutrals created at the target plates, now start towards the private flux region, and to prevent their immediate reionisation in the X-point region, a dome baffle has been installed between the target plates. Its base is transparent in poloidal direction (covering

about 40% of the area below the dome), allowing an exchange of the neutral reservoirs from both divertor legs.

Pumping now occurs from this private flux region, which is linked to the pump chamber by the finite conductance of the slit below the outer target plate (estimated to be about 45 m³/s). With the LYRA configuration, the 14 turbomolecular pumps with an effective pumping speed of about 12 m³/s (see Ref. [2]) have been supplemented by a cryo pump (see Ref. [3]), which is located behind the lower passive stabiliser (PSL), as shown in the lower part of Fig. 1. Therefore, its nominal pumping speed of about 100 m³/s is reduced to an effective pumping speed of about 32 m³/s in the divertor chamber below the dome baffle. It is foreseen to operate the cryo pump with Ar frosting to pump helium too, but presently it has been operated in the standard mode only, i.e. pumping deuterium/hydrogen and neon, but no helium. However, as the conductance below the outer target plate is much higher than the pumping speed of the turbo pumps, the effective pumping speed

^{*} Corresponding author. Tel.: +49 89 3299 1927; fax: +49 89 3299 2580; e-mail: bosch@ipp.mpg.de

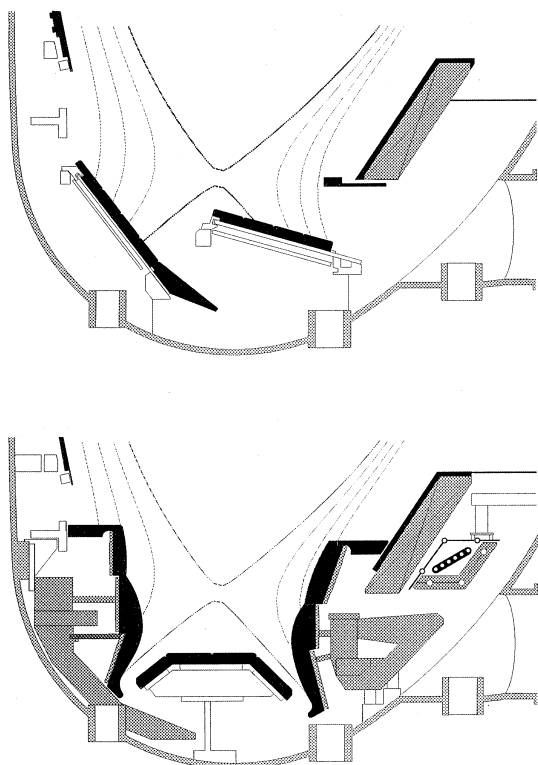


Fig. 1. Poloidal cross-section of the original ASDEX Upgrade divertor (DIV-I) in the top part of the figure and of the new LYRA configuration (DIV-II) in the bottom part. The target plates are built from three parts, the lower strike point module, which is hit by the separatrix with a small angle of incidence, the upper retention module, which follows the field lines parallel, but with some distance, and a transition module in between to connect both areas. The field lines in this figure have a radial distance of 12 mm in the plasma midplane.

for helium is hardly reduced, as compared with DIV-I. The pumping speed for neon has not yet been measured.

The detachment and core plasma performance of Divertor II compared with Divertor I are discussed in detail in Ref. [4], while this paper discusses specifically the differences in deuterium neutral gas behaviour and recent experiments on helium and neon exhaust in the LYRA divertor.

2. Deuterium neutral behaviour

The neutral gas behaviour in ASDEX Upgrade is measured with ionisation gauges [5] at different poloidal positions. For comparison of the divertor configurations we use a gauge in the main chamber midplane (no. 13), one in the private flux region (no. 1) and one in the pump chamber (no. 2). In DIV-I, the outer chamber was fed by the scrape-off layer, and the neutral gas reservoir

there dominated the divertor characteristics [2,6], while now the private flux region has taken over the role as divertor chamber. Therefore the divertor chamber in DIV-I is represented by gauge no. 2, and in Div-II it is represented by gauge no. 1. The bulk plasma parameters determining the neutral gas are the line average density \bar{n}_e in a horizontal channel through the plasma center, and the separatrix density measured by a lithium beam.

It has often been speculated that a tighter baffling of the divertor chamber could decrease the midplane neutral density (or the neutral flux density, which is proportional to the density, but a better parameter, as it is measured directly [2]) for given plasma parameters, and that this might improve plasma confinement. From our predictive modelling, however, no dramatic reduction of $\phi_{0,\text{main}}$ was expected, since the wall recycling was practically unchanged. In contrast, the tighter divertor should allow for higher $\phi_{0,\text{div}}$ [7].

Fig. 2 displays neutral flux densities in the main chamber and in the respective divertor chamber as a function of \bar{n}_e . The neutral flux density in the main chamber is rather similar in both configurations, as mentioned before. This was expected from B2/EIRENE modelling [7], because the neutral flux density in the main chamber is dominated by local recycling. Already for little baffling, the recycling neutrals determine $\phi_{0,\text{main}}$, and tighter baffling then will not decrease $\phi_{0,\text{main}}$ further. The divertor neutral flux density, however, is higher in DIV-II by a factor of about 4–5 for all densities. The dataset for DIV-II includes experiments with or without the cryo pump. If these subsets are separated, both $\phi_{0,\text{main}}$ and $\phi_{0,\text{div}}$ in DIV-II with the cryo pump active are 20% lower than without the cryo pump.

Fig. 3 compares the relation of main chamber and divertor neutral flux densities in both divertor configura-

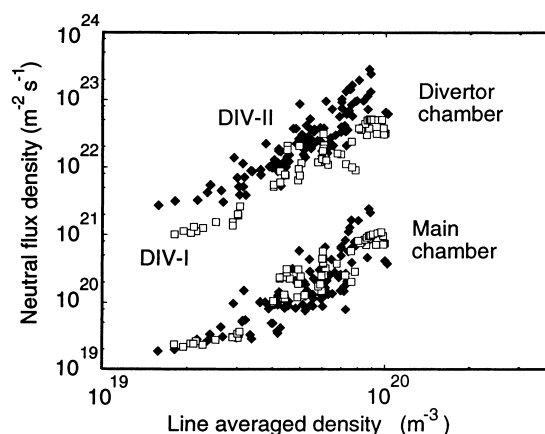


Fig. 2. Comparison of neutral flux densities in the main chamber (lower data points) and in the divertor chamber (upper points) as a function of \bar{n}_e . Solid symbols indicate data from DIV-II, open symbols those from DIV-I.

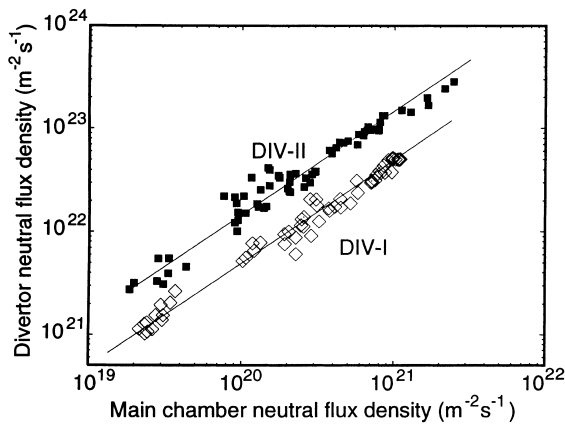


Fig. 3. Comparison of divertor neutral flux densities as a function of the main chamber neutral flux density in both divertor configurations. While in DIV-I the density ratio is about 30, it is about 170 in DIV-II. This dataset does not distinguish between the points with cryo pump (where the ratio is 155) and those without cryo pump, where the ratio is 180.

rations. In both cases the fluxes are proportional to each other, but while the compression ratio is about 30 in DIV-I, it is much higher in DIV-II, about 180 without the cryo pump, and 155 with the cryo pump. This again indicates very good neutral compression as a consequence of the tight divertor baffling.

3. Global helium exhaust

Helium puff experiments with DIV-I had shown that the exhaust rates increase with the divertor neutral flux density [8,2], and this was explained with 2d-modelling of scrape-off layer and divertor plasma [8,9]. From the exhaust rates in the DIV-I configuration one could derive the compression ratio ($C_{\text{He}} = n_{0,\text{div}}^{\text{He}} / n_{+, \text{edge}}^{\text{He}}$), but for the new configuration with the additional chamber (and some not well determined leakage paths) this can not be done so easily. Therefore an absolute He-density measurement in the exhaust gas is just taken into operation. The exhaust rate in this paper is determined from the decay rate ($1/\tau_{1/e}$) of a HeI line (at 588 nm) in the divertor.

As was seen in Fig. 2, $\phi_{0,\text{div}}$, which was a good parameter for particle exhaust in DIV-I, is now different for the same bulk plasma parameters. Fig. 4 compares exhaust rates in both divertor configurations as a function of \bar{n}_e , indicating much higher helium exhaust rates in DIV-II, while neon exhaust is considerably slower. The helium data for DIV-II include discharges with and without cryo pump, and both subsets overlap strongly, but the data with the cryo pump active tend to be higher. A specific comparison will be discussed in the next chapter.

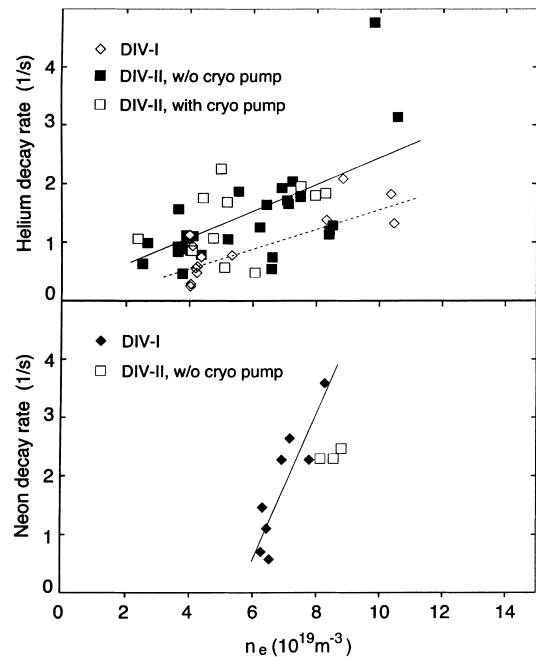


Fig. 4. Comparison of helium exhaust rates in both divertor configurations as a function of \bar{n}_e . This graph includes for DIV-II data points with and without cryo pump. Both these subsets overlap, although the exhaust rates with cryo pump tend to be on the upper side.

These faster exhaust rates for helium have been predicted by B2-EIRENE modelling [7], and can be understood from the geometry. The helium neutrals from the target plate are reflected towards the divertor chamber below the dome baffle, and since this chamber is well closed, they are retained and pumped. Also the slower neon exhaust was predicted [7], and is due to its smaller mean free path. A quantitative measure like the compression ratio for the trace impurities has not yet been determined for this configuration.

4. Helium exhaust with the cryo pump

Fig. 5 compares time traces for two similar discharges, one with the cryo pump active (#10276), and one without the cryo pump (#10275). The line averaged densities (feedback-controlled) are similar, but with the pump active, a much higher deuterium puff is necessary. With the pump active, $\phi_{0,\text{main}}$ and $\phi_{0,\text{div}}$ are much lower, and the deuterium compression ratio decreases. In both discharges small puffs of helium and neon were introduced, as indicated in Fig. 5. One finds that without the cryo pump, the neon exhaust rate (2.3/s) is higher than the helium exhaust rate (1.1/s), but in DIV-I this difference at such densities was much larger [2], as mentioned before. With the cryo pump active,

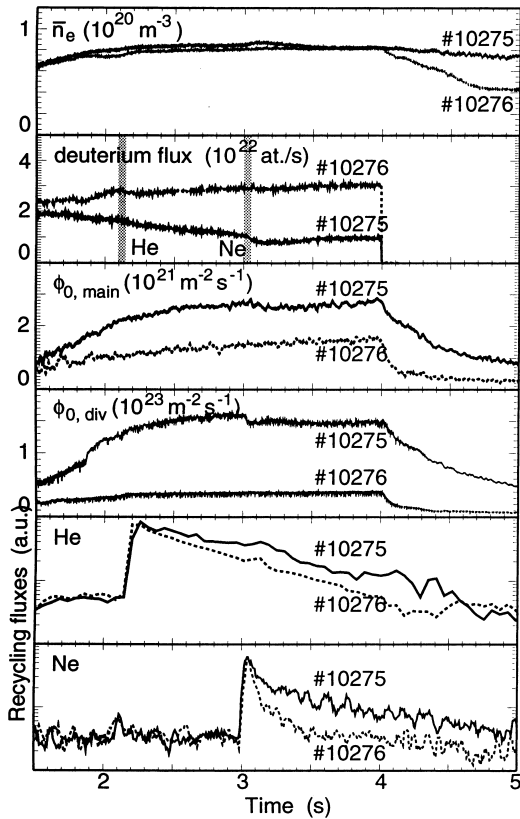


Fig. 5. Comparison of two similar discharges with (#10276) and without the cryo pump active (#10275). Neon is pumped by the cryo pump and its exhaust rate with the pump active is much higher. Helium is not pumped by the cryo pump, but as a much higher deuterium flow is necessary to keep the plasma density, this induced flow may enhance helium transport in the scrape-off layer.

both exhaust rates increase, especially for neon, because it is pumped by the cryo pump. For helium exhaust the effect of the pump is much smaller ($1.1/s \Rightarrow 1.7/s$), but clearly visible. In principle this can be due to deuterium flow induced scrape-off layer transport of helium, as it was observed in DIII-D [10,11]. However, the effect shown in Fig. 5 is much smaller than in DIII-D, where a deuterium flow of about 90 Torr l/s increases neon exhaust by a factor 3. This result is presently not fully understood and has to be confirmed in further investigations, especially including absolute density measurements of helium in the exhaust gas.

5. Influence of strike point position

The geometry of the LYRA requires all neutrals from the target plate to hit the slot below the dome to enter the divertor chamber. Once inside the chamber, the

conductance to the pumping chamber is larger than the conductance of this entrance slit, and the pumping probability therefore is high. Helium neutrals, with their rather large mean free path, will enter the divertor ballistically, and the probability for doing so decreases strongly with increasing distance of the recycling location to the divertor entrance (which means a decreasing solid angle). Therefore we expect a decrease in the He exhaust rate when moving the strike point upward. Deuterium neutrals, however, will always suffer many collisions, and they enter the divertor chamber independent of its exact location. These arguments have been confirmed by B2-EIRENE modelling [7].

Fig. 6 shows an experiment, where two discharges practically identical in density and energy content, are compared. In discharge 10618 both divertor strike points have been moved upward by 3 cm. This does not influence the deuterium compression, but the helium exhaust rate in this discharge is smaller by 35%.

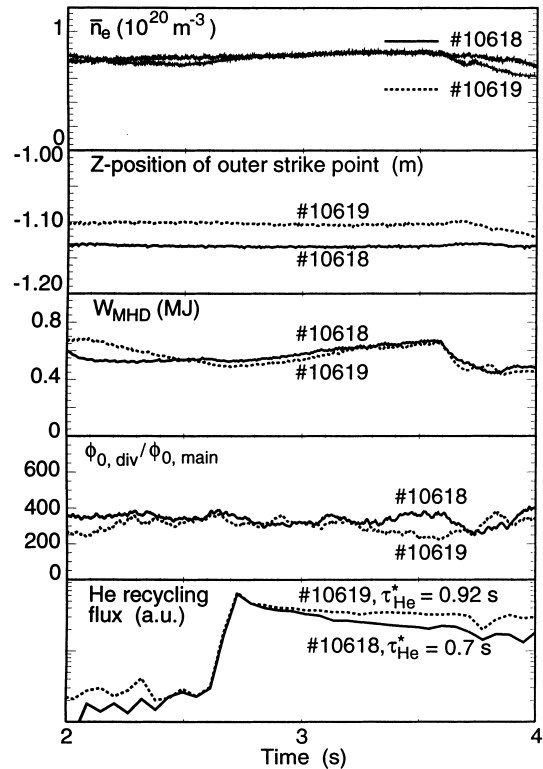


Fig. 6. Comparison of two similar discharges with the standard strike point position (#10618), and with an upward shift of 3 cm (#10619). Plasma shape (not shown), line averaged density and energy content are almost identical, as is the neutral compression ratio $\phi_{0,div}/\phi_{0,main}$. Helium exhaust, however, is about 35% slower in the upward shifted plasma, since the probability to hit the pumping slot decreases with the distance between strike point and slot.

6. Conclusions

As a result of the tight divertor baffling, the new LYRA-divertor in ASDEX Upgrade operates with a much higher neutral gas compression ratio, as compared with divertor I. As expected, however, this manifests itself in a higher divertor neutral density, while the main chamber neutral density has hardly changed. This is due to the wall recycling dominating the main chamber neutral gas reservoir.

As predicted from B2-EIRENE modelling, helium exhaust rates have increased, as compared with DIV-I, while neon exhaust is slower in DIV-II.

The helium exhaust rate is increased also, when the cryo pump is used to induce external (deuterium) particle flow. This is similar to DIII-D, where ‘puff and pump’ increases impurity exhaust strongly, but the effect is much smaller, and in contrast to results in DIV-I, where such an effect was never observed [6]. These results clearly need further investigations.

When the plasma is shifted upwards, with the strike points hitting the target plate further away from the entrance slit to the divertor, the helium exhaust rate decreases, while the deuterium neutral gas compression is hardly influenced. This is due to ‘ballistic’ pumping of helium, as predicted by B2-Eirene modelling [4,7].

References

- [1] H.-S. Bosch, D. Coster, S. Deschka, W. Engelhardt, C. García-Rosales et al., Technical Report 1/281a, IPP, Garching, Germany, 1994.
- [2] H.-S. Bosch, D. Coster, R. Dux, G. Haas, A. Kallenbach et al., *Plasma Phys. Controlled Fusion* 39 (1997) 1771.
- [3] B. Streibl, S. Deschka, O. Gruber, B. Jüttner, P. Lang, et al., in: C. Varandas, F. Serra (Eds.), *Fusion Technology (Proceedings of 19th Symposium on Fusion Technology, Lisbon, 1997)*, Elsevier, Amsterdam, vol. 1, 1997, pp. 427–430.
- [4] R. Schneider, H.-S. Bosch, D. Coster, J. Fuchs, J. Gafert et al., these Proceedings.
- [5] G. Haas, J. Gernhardt, M. Keilhacker, E.B. Meservey, ASDEX Team, *J. Nucl. Mater.* 121 (1984) 151.
- [6] H.-S. Bosch, R. Dux, G. Haas, A. Kallenbach, M. Kaufmann et al., *Phys. Rev. Lett.* 76 (1996) 2499.
- [7] R. Schneider, H.-S. Bosch, J. Neuhauser, D. Coster, K. Lackner et al., *J. Nucl. Mater.* 241–243 (1997) 701.
- [8] H.-S. Bosch, D. Coster, R. Dux, C. Fuchs, G. Haas et al., *J. Nucl. Mater.* 241–243 (1997) 82.
- [9] R. Schneider, D. P. Coster, K. Borrass, H.-S. Bosch, J. Neuhauser et al., *Plasma Physics and Controlled Nuclear Fusion Research, IAEA, Vienna*, vol. 2, 1997, pp. 465–476.
- [10] M.J. Schaffer, D.G. Whyte, N.H. Brooks, J.W. Cuthbertson, J. Kim et al., *Nucl. Fusion* 35 (1995) 1000.
- [11] M.J. Schaffer, M.R. Wade, R. Maingi, P. Monier-Garbet, W.P. West et al., *J. Nucl. Mater.* 241–243 (1997) 585.